The Astrophysical Journal, 808:131 (10pp), 2015 August 1 doi:10.1088/0004-637X/808/2/131

PRESSURE SHIFT AND GRAVITATIONAL REDSHIFT OF BALMER LINES IN WHITE DWARFS: REDISCUSSION*

Jacek Halenka[1], Wieslaw Olchawa[1], Jerzy Madej[2], and Boleslaw Grabowski[3]
[1] Institute of Physics, University of Opole, ul. Oleska 48, 45-052, Opole, Poland; halenka@uni.opole.pl, wolch@uni.opole.pl
[2] Astronomical Observatory, University of Warsaw, Al. Ujazdowskie 4, 00-478 Warszawa, Poland; jm@astrouw.edu.pl
[3] Wroclaw School of Information Technology WWSIS "Horyzont," ul. Wejherowska 28, 54-239 Wroclaw, Poland; bgrab@uni.opole.pl
Received 2015 February 21; accepted 2015 June 8; published 2015 July 27

ABSTRACT

The Stark-induced shift and asymmetry, the so-called pressure shift (PS) of H_α and H_β Balmer lines in spectra of DA white dwarfs (WDs), have been examined in detail as masking effects in measurements of the gravitational redshift in WDs. The results are compared with our earlier ones from a quarter of a century ago. In these earlier papers, the standard, symmetrical Stark line profiles, as a dominant constituent of the Balmer line profiles but shifted as a whole by the PS effect, were applied to all spectrally active layers of the WD atmosphere. At present, in each of the WD layers, the Stark line profiles (especially of H_β) are inherently asymmetrical and shifted due to the effects of strong inhomogeneity of the perturbing fields in plasma. To calculate the Stark line profiles in successive layers of the WD atmosphere we used the modified Full Computer Simulation Method, able to take adequately into account the complexity of local elementary quantum processes in plasma. In the case of the H_α line, the present value of Stark-induced shift of the synthetic H_α line profile is about half the previous one and it is negligible in comparison with the gravitational redshift. In the case of the H_β line, the present value of Stark-induced shift of the synthetic H_β line profile is about twice the previous one. The source of this extra shift is the asymmetry of H_β peaks.

Key words: atomic processes – line: formation – line: profiles – plasmas – white dwarfs

1. INTRODUCTION

A quarter of a century has passed since we found out for certain that the Stark-induced shift and asymmetry effects (hereafter called the "pressure shift," PS), caused by local atomic quantum processes in plasmas, play an important role in the formation of the Balmer hydrogen lines in the spectra of white dwarfs (WDs), and that the contribution of PS to the residual (free of the Doppler component) redshift of these lines must be taken into account while separating the gravitational (Einstein's) redshift. We find the first note on that theme in the papers by Wiese & Kelleher (1971) and Wiese et al. (1972). They experimentally revealed slight systematic shifts of these Stark-broadened lines to the red, which are linear functions of the electron density. They used hydrogen plasma as the source of light—an environment similar to that in WD atmospheres. Moreover, the measurements were taken in the same way as those in the WD spectra in two pioneering papers by Greenstein & Trimble (1967) and Trimble & Greenstein (1972), where the gravitational redshifts were determined within the relatively broad central region of a Balmer line—the so-called "averaged line center" (ALC)—in the best spectra available at that time, i.e., in those recorded by means of a 508 cm telescope.

The results of the determination of gravitational redshifts by Greenstein and Trimble for WDs revealed an unexpected and surprising problem, which in time was called *the astrophysical puzzle* (cf. Weidemann 1979): for some unknown reasons, the measured (residual, i.e., free from the Doppler component) WD redshifts were systematically too great, by up to about 50% (10–15 km s^{-1} in Doppler velocity units), exceeding predictions by Einstein's General Relativity. (More precisely: WD masses resulting from the gravitational redshift measurements systematically exceeded those determined using the so-called astrophysical methods, i.e., an astrometric one, model atmospheres, and so on.) Wiese & Kelleher (1971), in their significant paper entitled "On the cause of the redshifts in white-dwarf spectra," noted a propos: "It appears that the Stark-induced redshift accounts for a portion of the observed redshift in WDs which has previously been attributed entirely to gravitation."

At that time, the appearance of the Stark-induced redshift was surprising indeed, because splitting of Balmer lines in external homogeneous electric fields, as observed in those days in laboratories, was symmetrical. The quadratic Stark effect (QSE) generates line shifts (usually to the red) and line asymmetry. "However,"—we quote Wiese & Kelleher (1971) again—"based on all the then available experimental and theoretical knowledge—the work of Rausch von Traubenberg & Gebauer (1929a) and Griem (1964) is especially cited—the Stark shifts were estimated to be insignificant."

In both objects under consideration—in the WD spectra and in the light of the device (the high-current, wall-stabilized arc) of Wiese & Kelleher (1971) type—the hydrogen Balmer lines are enormously broadened by the interparticle Stark effect in plasma. In both cases also, these lines appeared, for a long time, to be practically symmetrical and unshifted, contrary to the so-called "metal" lines of all heavier atoms—narrow and easy to measure, but strongly affected by Stark shift and asymmetry. These last ("metal") lines are completely useless for the purpose of the gravitational redshift measurements. For about four decades now it has undoubtedly been a well-known fact that the Stark-broadened hydrogen Balmer lines in dense plasma[4] are—apart from their huge broadening—slightly

* In memory of Jan Jerzy Kubikowski (1927–1968)—one of the pioneers of plasma in astrophysics.

[4] One routinely reads the term "dense plasma" (or "high-density plasma") as a plasma of electron concentration about and above 10^{16} cm^{-3}. For example, in the paper by Wiese et al. (1972), entitled "Detailed study of the Stark broadening of Balmer lines in a high-density plasma," investigations cover the range of electron densities N_e between 1.5×10^{16} and 10^{17} cm^{-3}. In WD atmospheres, the range of N_e is usually considerably broader.

asymmetrical and redshifted as well. The asymmetry and redshift are effects of relatively small size but phenomenally, in their physical specification, very complicated. Detailed measurements and a careful theoretical balance of physical processes forming the hydrogen spectral lines in plasma lead us step by step to a complete understanding and a successful description of the Stark-induced shift. So, the Stark-induced shift, as a masking effect, can be definitely separated from the gravitational redshift measurements in the WD spectra.

The first simple attempt to provide a theoretical explanation of the effect discovered by Wiese & Kelleher (1971) and Wiese et al. (1972) in the hydrogen Balmer lines in plasma was made by Grabowski & Halenka (1975)—as a specific consequence of Debye screening, i.e., the neutralizing action of a negatively charged plasma background on the atomic nucleus, and of the resulting deformation of the internal structure of disturbed hydrogen atoms. The result, PS $\propto N_e/T$ (for details see that reference), was surprisingly fair: the predicted PS of the line center to the red became evident and was of the same order of magnitude as the observed excess over gravitational redshift. In the recapitulating paper by Grabowski et al. (1987), we calculated the synthetic Balmer line profiles in WD spectra for a wide range of $\log g$ and $T_{\rm eff}$ values of WD atmospheres in a physically more realistic approach, corresponding to the world state of the art in the hydrogen-spectral-line broadening theory of that time (see Section 3). We used, namely, symmetrical Stark-broadening line profiles (following Edmonds et al. 1967) as functions of the local physical conditions in successive layers of a stellar atmosphere; moreover, in each layer the line profile was shifted as a whole by the value of the PS, depending on the proper local physical condition in the layer. The PS function was calculated, taking into account complex influences of the plasma environment on a H atom: (1) the predominant effect—the screening of the atomic nucleus by the cloud of free electrons, following Grabowski & Halenka (1975), but corrected empirically (by a multiplicative factor), according to the laboratory data accessible at that time, and (2) the phenomena of the correcting nature (especially in the case of the H_β line), caused by the resultant quasistatic local ionic field. We took into consideration the following contributions: multipole expansion (ME) of the perturbing fields, including the quadrupole term, and the second-order corrections of the ionic field to the frequency shift (QSE). The first-order correction in the alterations of the oscillator strength of the line components, and the so-called pressure ionization in plasma, have also been taken into account (for details see Grabowski et al. 1987).

The principal results were as follows: asymmetry and PS (to the red) of the synthetic Balmer line increase with the distance from the line center; the H_β line is strongly affected by PS and, consequently, is less useful for the determination of gravitational redshift, especially when far wings are used to define the ALC. The relative significance of the PS of Balmer lines, as compared with Einstein's gravitational redshift, systematically decreases with increasing values of $T_{\rm eff}$ and of $\log g$—from about 50% of the gravitational redshift down to about a mere 1%—at both opposite poles, i.e., at extremely low and extremely high values, respectively (cf. Madej & Grabowski 1990).

Today, over a quarter of a century later, when excellent, high-resolution spectroscopic data, with clearly revealed, sharp, non-LTE line centers of Balmer lines are accessible from the

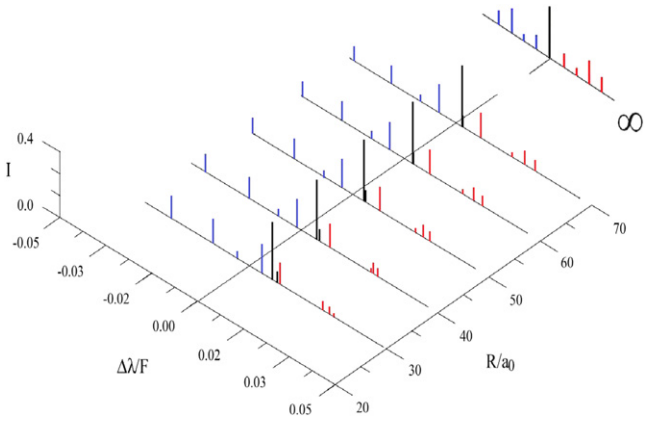

Figure 1. Quasistatic Stark spectrogram (pattern of splitting) of the H_α Balmer line, as an example, in the field of a single, fixed ion, as a function of the ion–atom distance R, expressed in the reduced scale R/a_0, where a_0 is the Bohr radius; at (formally) $R/a_0 = \infty$ (in the homogeneous perturbing electric field) —the canonical picture of the linear Stark effect (LSE) splitting. The distance from the line center is expressed on a reduced scale (in the denominator there is the field strength in the corresponding ion–atom distance). The blue and red components are marked by these colors, the central component by black.

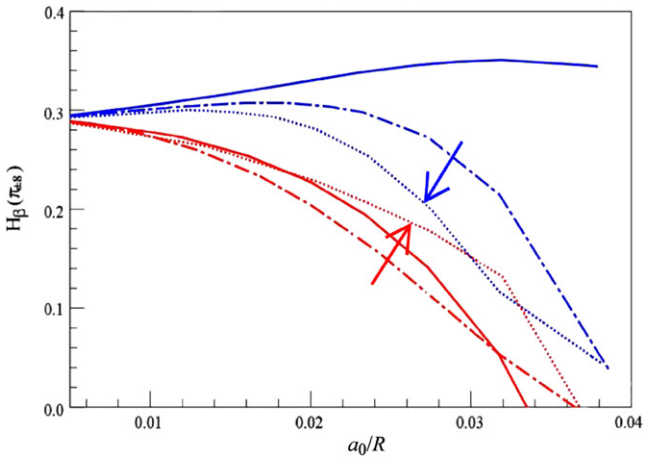

Figure 2. Evolution of the intensity of selected Stark components of the H_β line as a function of the reciprocal ion–atom distance in different approximations. See text for details. The blue and red components are marked by these colors.

Hubble Space Telescope (*HST*; e.g., Barstow et al. 2005), ESO (e.g., Falcon et al. 2010), or Very Large Telescope (VLT) (e.g., Casewell et al. 2009), the importance and usefulness of these old, above-discussed, results on PS are rather archival. At present we are able to calculate the synthetic WD Balmer line profiles with incomparably higher precision, taking into account a more complete description of the quantum physical processes that are active in the creation of WD Balmer lines. (For comment on the specific phenomena active in the creation of PS and asymmetry of Balmer lines in plasma, taken into account in the present calulations, see Section 2, the second through the last paragraphs, especially the visualization in Figures 1 and 2, and also in Section 3, the third and fourth paragraphs.)

Measurements of the gravitational redshift give WD masses (specifically the mass/radius ratio) immediately and with the highest exactness (of the same order as—in the incidental cases —the orbital astrometry of binary systems), practically

independently of anything—under the condition, however, that the spectral measurements are free of (separated from) disturbing and masking effects produced by mixed up elementary processes in the plasma of WD atmospheres, especially at low values of $\log g$ and $T_{\rm eff}$. We devote our paper to improving the reliability of this excellent method. Activity in that direction is desired and expected (see, e.g., Koester 1987; Provencal et al. 1998; Barstow et al. 2005; Falcon et al. 2010). We will discuss relevant problems in next sections.

2. AN INTRODUCTORY NOTE ON THE ELEMENTARY PHYSICAL PROCESSES FORMING THE BALMER LINE PROFILES IN PLASMA (IN WD ATMOSPHERES IN PARTICULAR)

One cubic centimeter in a sample layer of a typical WD atmosphere, at a temperature of the order of 10,000 K, contains about 10^{20} atoms; almost all are hydrogen ones, of which one in a thousand is an ionized atom, i.e., without a bound electron. So, in that volume we meet about 10^{17} electric charges (electrons and ions). The electric field attached to a charged particle is a long-range one ($\sim r^{-1}$), therefore each charged particle acts simultaneously on lots of other charges and neutrals. All particles move with great velocities, of hundreds/thousands of meters per a second. On the scale of nanoseconds (the typical clock beat for atomic microprocesses), the influences of ions (slow) are nearly constant, resulting in quasistatic splitting of the atomic levels into sets of sublevels; the perturbations by electrons (fast) are rapidly changing, and are "seen" by atoms as impacts, resulting in a reduction of lifetimes and in broadening of the atomic sublevels. Moreover, mutually overlapping field strengths reduce the scope of this field penetration (the so-called screening effects). This is a typical scenario of line profile formation in the plasma conditions.

To start, we consider the simplest, virtual case: a single ion (proton) at rest, acting on a tentative hydrogen atom, also fixed, dependently on the distance between these particles. We temporarily ignore all the remaining charged particles. This pair of particles (called the nearest neighbor approximation) stands for an extremely simplified physical quantum system, but the mathematical problem of solution of the corresponding time-independent perturbation theory (PT) is by no means simple (cf. Olchawa et al. 2001, and Figures 1 and 2 therein, and below).

Figure 1 presents the solution for the Balmer-α line as an example. In the homogeneous external electric field (in our demonstrative model of the perturbing point charge, the homogeneous field formally corresponds to the infinite distance of the perturber) the splitting of line components is strictly symmetrical (see the upper-right corner of the figure). This is the canonical pattern of the linear Stark effect (LSE) of Balmer-α in a homogeneous external field. The field of the perturbing ion is, of course, the more inhomogeneous, the nearer the ion resides (the ion–atom distance is expressed in R/a_0, where a_0 is the Bohr radius) and, consequently, the ME (some kind of Taylor series) of the perturbing field strength must be taken into account in the calculations, i.e., the dipole term (corresponding to the homogeneous component), a quadrupole one (the first-order correction), an octupole one (the second-order correction), and so on, if necessary. In the case under examination, all these higher order multipole terms have been taken into account. We see the effect of these terms on the line splitting in the changes in location (and even in succession!) and in intensities of the line components. In particular, the intensities of the red components (the right-hand side of the figure, when we are looking toward the LSE pattern) decrease with the decreasing ion–atom distance, but all line components move to the red—creating a complicated image of the pressure asymmetry and shift formation.

In Figure 2, the evolution of the intensities of the selected Stark components of the H_β line is presented. As a sample, the strongest (π_8) Stark components are used: π_{-8} (the blue component, the upper curve of a given style in the figure) and π_{+8} (the red component, the lower curve in the figure) as a function of the reciprocal reduced distance (a_0/R), showing their dependence on the approximation used. The styles of curve used have the following meaning: solid lines—dipolar perturbation (homogeneous external field), the QSE is included; short-dashed curves—the quadrupole interaction is also included; dotted curves—the octupole interaction is also included. The evolution presented by the dotted curves (marked by arrows) is the most precise.

In Figure 1 and, especially, Figure 2, we see that the main source of asymmetry—and of the asymmetry-induced shift—in the quasistatic approximation is the inhomogeneity of the ion microfield in the surroundings of an atom that is active in the spectral line formation: the quadrupole and the octupole terms, and also the QSE.

3. CALULATIONS OF THE STARK PROFILES OF HYDROGEN LINES IN A PLASMA ENVIRONMENT

The fundamental principles of the Stark-profile calculations of hydrogen lines formed in plasma environments were formulated in the 1950s in the pioneering papers by Baranger (1958), and in the 1960s by Hans R. Griem and his coworkers (Griem et al. 1962). In the so-called generalized impact-broadening theory, formulated at that time, the influences of fast moving electrons perturb, as impacts, a hydrogen atom and reduce the lifetime (causing broadening) of sublevels (separated and well defined in the quasistatic ion field) of both the upper and lower levels of the line. A complete Stark profile is a result of an averaging of impact profiles created in such a manner over the quasistatic ion field strengths within the Debye sphere (some "interacting volume" of plasma around an atom, limited by effects of mutual screening of the charged particles). The best sources of Stark profiles of those days were those by Griem (1964, 1974) and Kepple & Griem (1968), generally known as "modified impact theory." Nearly equivalent ones are: the "unified theory" by Vidal et al. (1973) and "semiempirical profiles" by Edmonds et al. (1967). They include the Debye shielding effects of the perturbing ions, but the ions everywhere are treated as static ones (the thermic ion dynamics is omitted generally), and, furthermore, the Stark splitting caused by ions is assumed as LSE entirely—a symmetrical and unshifted one—i.e., the higher order corrections in the ME, and in the PT (the second-order PT correction gives the QSE), are completely neglected. In all these calculations, the classical path approximation (CPA; assuming that the perturbing electrons move along the classically specified paths) is always used. Fortunately, the CPA is entirely satisfactory in most applications (e.g., Griem 1974) and does not demand improvement. Neglecting the ion dynamics, however, creates serious uncertainty in the line centers—in the region of special importance for gravitational

redshift measurements. An extreme defect—from the point of view of the gravitational redshift measurements in WD spectra—of the quasistatic approaches in the majority of existing Stark-profile theories lies in the complete neglect of the higher order corrections in the Hamiltonian (ME) and in PT, as well. It is these corrections that produce the redshift and asymmetry features in the hydrogen line profiles observed in spectra of moderately dense and very dense plasmas, and, naturally, appearing in the WD spectra, too.

The spectral line shapes, particularly the hydrogen line shapes, are one of the most important carriers of information on the structure of laboratory plasmas, as well as space plasmas. From the astrophysical point of view, this refers mainly to the plasma of stellar atmospheres and the plasma of WD atmospheres particularly. In order to get reliable recognition of the physical features of the investigated plasma environment (i.e., in order to get the plasma diagnostics) through the line-shape analysis, the line shapes must be calculated with sufficient accuracy. To attain this, different approaches are accepted—analytical methods and computer codes of various complexity and accuracy, and of different limits of applicability. The reader interested in this subject can find more information on the line broadening in recent reviews, e.g., by Günter & Könies (1997), Djurović et al. (2009) and in papers quoted therein. In particular, one can find a review of the line profiles obtained by using the so-called Full Computer Simulation Method (FCSM) compared with other approaches in the paper by Ferri et al. (2014).

The line shape and/or the line width (FWHM, in particular) serves the purpose of plasma diagnostics, as the main source of information on the physical properties of a diagnosed medium. FCSM approaches (Gigosos & Cardenoso 1989, 1996; Halenka & Olchawa 1996) very faithfully reconstruct the local phenomena in plasma and, consequently, give the shape and width of the line relevant to this aim. These approaches, however, are able to predict neither asymmetry nor a shift of the line.

We refer briefly to the principle of FCSMs. The local ionic, as well as electronic, shares in the spectral line formation are allocated using the simulation method, and the time-dependent Schrödinger equation is solved numerically. The ionic contribution is, as a rule, limited to dipole interaction of the atom–ionic field, and to the first-order correction in PT, i.e., to the LSE only. The resulting line profile is therefore a symmetrical and unshifted one. However, the FCSMs have no limitations present, e.g., in the theories of Kepple & Griem (1968) and Vidal et al. (1973), i.e., quasistatic ion fields, nor an impact approximation for free electrons. The quadrupole interactions (the first-order correction in the ME) as well as the QSE (the second-order correction in PT) can indeed be taken into account in FCSM—see paper by Olchawa (2002). Such an improved approach leads to the effects of line asymmetry and to the Stark-induced shift—to effects important especially in conditions of dense plasma. These predictions excellently agree with recent laboratory measurements. Unfortunately, this improved approach is very time-consuming, and a laborious one. We, therefore, have developed an equally reliable, but more effective method, useful in efficient line profile calculations, when a wide range of different physical conditions (successive layers of the WD atmosphere) must be examined. Here the shape of the spectral line is a sum of two components. The first component (of the zeroth-order term in PT and the first in ME, i.e., LSE in the dipole approximation) is calculated using the FCSM approach. The second component (consisting of a variety of corrections, each small compared to the first component) includes the contributions originating from higher order terms of the emitter–ionic microfield interactions (the quadrupole interactions and QSE, calculated in the quasistatic approximation for ions). This second component describes the shift and asymmetry of the Balmer line profile produced by the ion constituent of plasma. The shifts caused by electrons have been taken into account, following the paper by Griem (1983). The method used—modified FCSM (in our notation, mFCSM)—is an effective one, producing realistic line profiles that are broadened, shifted, and asymmetrical, agreeing, moreover, with the laboratory measurements. This method has been formulated in a series of papers by Halenka & Olchawa (1996), Olchawa (2002), Wujec et al. (2002), and Olchawa et al. (2004), and, finally, was successfully examined and improved in the paper by Griem et al. (2005). All the calculations of the hydrogen line profiles in the present paper have been carried out following this mFCSM method.

Particular problems, related to the matter in the hand, have been solved in the following references: a detailed discussion and proper quadrupole and octupole corrections of the ionic fields, producing asymmetry and redshift of the Stark line profile in plasma—in a series of papers by Halenka and Olchawa: Halenka (1990), where correction of the "modified impact theory" was made, including the emitter–ion quadrupole interactions, the QSE, and the ion dynamics effects; Halenka & Olchawa (2007)—octupole inhomogeneity tensor of ionic microfield in Debye plasma at a neutral emitter, calculated for the first time; Halenka (2009)—the octupole inhomogeneity tensor at an ionized emitter, also calculated for the first time.

The starting point of this consideration is the relation between the spectral line profile and the average of the dipole autocorrelation function $C(t)$, which can be written in the following way:

$$I(\Delta\omega) = \lim_{t_f\to\infty} \pi^{-1} \int_0^{t_f} C(t) e^{i\Delta\omega t} dt \tag{1}$$

$$C(t) = \mathrm{Tr}\{\boldsymbol{d}_{if} \cdot U^{\dagger}_{ff'}(t) \boldsymbol{d}_{f'i'} U_{i'i}(t)\}_{\mathrm{av}} \Big/ \mathrm{Tr}\left\{\boldsymbol{d}_{if} \cdot \boldsymbol{d}_{fi}\right\}, \tag{2}$$

where $\boldsymbol{d}$ is the dipole operator for the hydrogen atom, while ii' and ff' indicate the sublevels of the initial (E_i) and final (E_f) states of the unperturbed atom, respectively. The frequency separation from the line center is given by $\Delta\omega = \omega - (E_i - E_f)/\hbar$; $U(t)$ is the operator of the time development of the hydrogen atom in the presence of the electric field produced by electrons and ions. The averaging $\{\cdots\}_{\mathrm{av}}$ is taken over all initial simulated field strengths and possible time histories. The time-evolution operators $U_{i'i}(t)$ and $U^{\dagger}_{ff'}(t)$ (corresponding to the initial and final states, respectively) satisfy the following Schrödinger equation:

$$i\hbar\dot{U}(t) = \left[H_0 + V(t)\right] U(t), \tag{3}$$

where H_0 is the Hamiltonian of the isolated radiator and $V(t)$ is the radiator–plasma interaction potential. The Hamiltonian, with the ME of the potential restricted to quadrupole terms,

may be written, e.g., Halenka (1990), as follows:

$$H(t) = H_0 - \boldsymbol{d} \cdot \boldsymbol{F}(t) - 1/6 \sum_{jk} Q_{jk} F_{jk}(t) + \cdots, \qquad (4)$$

where the second term in Equation (4) describes the plasma–emitter dipole interaction and the third represents the quadrupole interaction of the radiator with the inhomogeneous electric microfield of the plasma. The electric field $\boldsymbol{F}(t)$ and the inhomogeneous microfield tensor $F_{jk}(t)$ represent the respective total fields originating from ions and electrons.

We computed a pure H model atmosphere of typical WD parameters: $T_{\rm eff} = 12{,}000$ K (in figures below we use the abbreviation 12 kK) and log $g = 8.0$ (cgs units) using the ATM computer code. Synthetic Balmer line profiles were computed using our LINE code, which was derived from the ATM program. Both codes solve the equation of state in gas, assuming local thermodynamic equilibrium (LTE) and were described by Madej (1983). They are practically the same as in papers by Grabowski et al. (1987), hereafter ApJ'87, and Madej & Grabowski (1990), hereafter A&A'90, but were modified for the purposes of the present paper. Numerical accuracy of the ATM code is high, since it ensures that error of the bolometric radiation flux is much less than 1% across the WD model atmosphere. Both high accuracy and the physical foundations of these codes (the requirement of hydrostatic and radiative equilibrium) are comparable with other computer programs for model atmospheres used routinely nowadays, e.g., the computer code TLUSTY Version 195 (Hubeny 1988; Hubeny & Lanz 1997) in its basic component, modeling a plane-parallel, horizontally homogeneous stellar atmosphere in radiative and hydrostatic equilibrium. LINE, which is a program for calculating the spectrum emerging from an ATM model atmosphere, is comparable to the program SYNSPEC Version 43 (Hubeny & Lanz 2000). The only serious simplification is the LTE solution of the equation of state. Therefore, both ATM and LINE codes are suitable for differential investigations of the features of the synthetic Balmer line profiles, when our interest is focused on testing of two Stark opacity functions, distinctly differing from each other.

Our model atmosphere of the sample WD consists of 49 gas layers of various optical and geometrical depths. The coolest (shallowest) layer has temperature $T = 5500$ K and electron concentration about $N_{\rm e} = 1.5 \times 10^{10}$ cm^{-3}, whereas the deepest (hottest) one contributing to the synthetic hydrogen spectral line profile has $T = 55{,}000$ K and $N_{\rm e} = 2 \times 10^{18}$ cm^{-3}. For each layer of the WD model atmosphere we calculated complete Stark line opacity profiles, which were broadened, asymmetrical, and shifted as the result of all relevant physical processes in plasma, including motion and shielding of perturbing ions plus the Stark–Doppler coupling (not only convolution, but also dependence). For this purpose we applied the modified FCSM.

4. VERIFYING THE THEORETICAL CALCULATIONS

In order to check the calculations of the complete—broadened, asymmetrical, and shifted—Stark profiles of the Balmer-α and Balmer-β lines in the proper range of physical conditions of fixed, homogeneous, thin-layer plasmas, we have carried out verifying experimental measurements. For the purpose of this study we have applied the same experimental device of the plasma generation (a high-current wall-stabilized arc), the light treatment, and the smoothing procedure of the spectral recordings, as those described in earlier papers: Wujec et al. (2002) and Griem et al. (2005). Specific data of the experiments were nearly the same as in the paper by Griem et al. (2005)—with differences concerning the working gas (argon–hydrogen mixture in the cited reference) and the method of the plasma diagnostics (LTE), as follows: (1) As a plasma material we have used nearly pure argon, with a small admixture of atomic hydrogen gas. (2) The pLTE (partial LTE) plasma diagnostics have been applied.

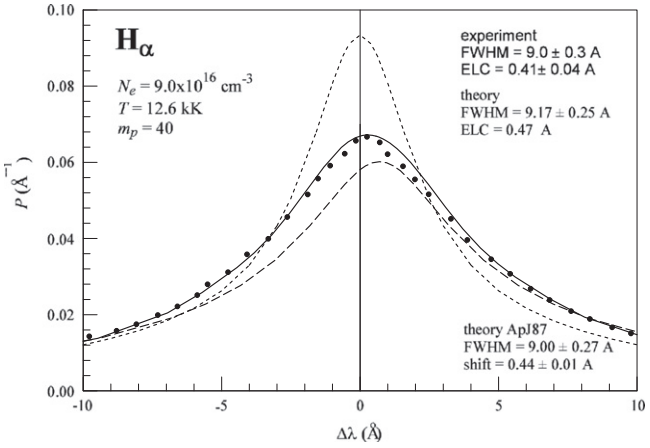

Figure 3. Comparison of the H_α line profiles of different references and meanings in the given physical conditions of plasma ($m_p = 40$—the atomic mass of argon). See the text for details.

In the cylindrical channel of the discharge arc, working at atmospheric pressure, the argon plasma is very stable, of nearly perfect cylindrical symmetry, and homogeneous along the lines of view parallel to the arc axis. The argon plasma, with a small admixture of hydrogen, acquires features of high-density plasma, and, at the same time, the plasma is an optically thin layer in hydrogen lines. T and $N_{\rm e}$ values are extremely high along the symmetry axis of the arc channel, and decrease with the radial distance from the axis. In the paper of Griem et al. (2005), we diagnosed plasma conditions assuming LTE. In the present paper, however, we carried out—more careful and realistic—pLTE plasma diagnostics, i.e., we adopted: modified Boltzmann and Saha–Eggert laws, Dalton's law and the electrical neutrality of the plasma. We took the integral emission coefficients of Ar I 4300 Å and H_α or H_β from the experiment. We have taken the overpopulation factors of Ar I ground level for pLTE diagnostics from the paper by Helbig & Nick (1981). The experimental investigations have been performed at plasma electron densities between 2.8 and 10.0×10^{16} cm^{-3}. Some results of the experiments are visible in Figures 3–6, as an example. In the matter of PS and asymmetry of the investigated Balmer lines, we obtained an excellent agreement of the experimental and the calculated data.

In Figure 3, the Stark line profiles of H_α are compared. The black points are the experimental data of the present paper; the long-dashed curve shows the same theoretical approximation as that used in our paper ApJ'87—symmetrical Stark profile following Edmonds et al. (1967, hereafter ESW) but shifted as a whole, as a function of the physical conditions of plasma in the given layer of the WD atmosphere; the short-dashed curve is the Stark line profile by Vidal et al. (1973, hereafter VCS)—a symmetrical and unshifted one; this approximation is the

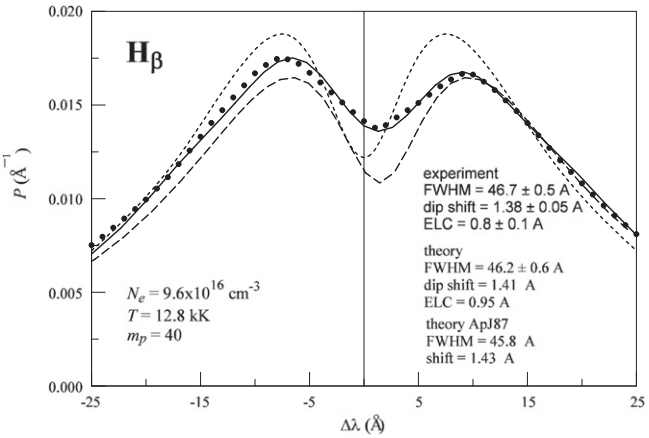

Figure 4. Comparison of the H_β line profiles of different references and meanings in the given physical conditions of plasma. The symbols and the curves used have the same sense as in Figure 3. The central dip displayed on the line profiles represented by the dashed curves is too deep. This defect is a consequence of neglecting the ion dynamics. The agreement of the measured and the calculated mFCSM data is excellent.

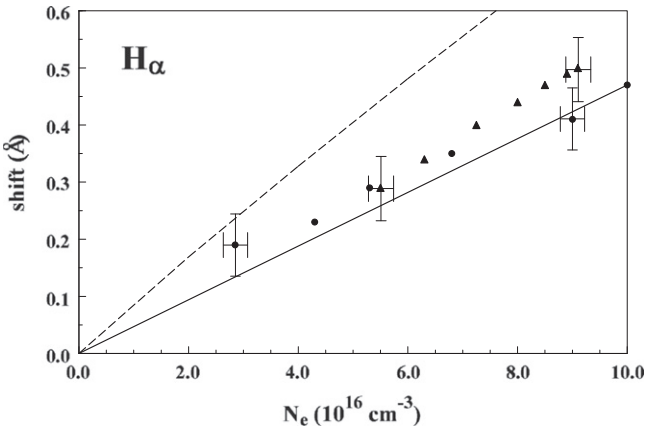

Figure 5. Pressure shift (PS) to the red of the peak of the H_α line as a function of the electron concentration in plasma. The dashed curve is the PS as in ApJ'87; the solid curve is the PS of our present calculations using mFCSM; the black triangles show measurements by Wiese et al. (1972) and the full circles are our measurements, both according to the paradigm of ELC.

main one in astrophysical spectroscopy (e.g., Barstow et al. 2005); the solid curve is our modified FCSM, complete Stark line profile of Balmer H_α, asymmetrical and shifted to the red. We see particularly that: (1) the agreement of our calculated (using mFCSM) and measured Stark line profile of Balmer H_α is perfect; (2) ESW—shifted (ApJ'87)—the line profile runs correctly; (3) VCS line profile has a defectively described line center, and is not suitable for WD applications.

The FWHM of the line and the redshift of the "experimental line center" (ELC, as defined by Wiese & Kelleher 1971) of the experimental line profile and of the modified-FCSM one are also shown in the figure. The agreement of these data in the case of the H_α line, as well as the H_β line (Figure 4), is excellent. We would like to focus on the PS of the H_α line peak —it is a little smaller in the experimental and modified-FCSM line profiles than that in paper ApJ'87, similarly as in the case of the H_β line, discussed in detail in Figures 5 and 6.

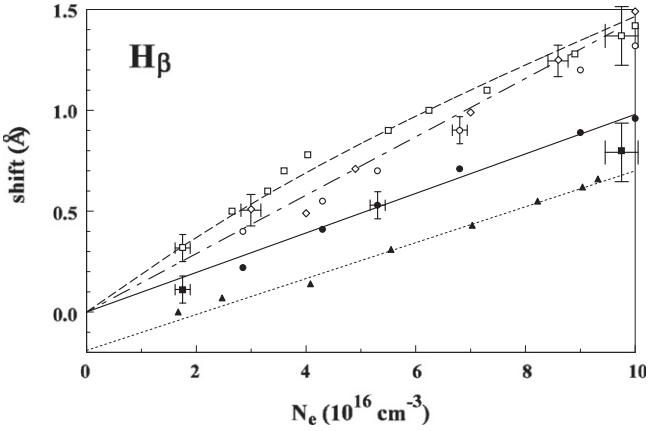

Figure 6. Pressure shift (PS) to the red of the central dip of the H_β line as a function of the electron concentration in plasma. The lines and the symbols have the following meanings: the black triangles and the dotted line are the original experimental measurements of the ELC and the proper best fit, respectively, by Wiese et al. (1972); the solid line and full circles are the ELC-type redshifts, calculated (via mFCSM) and measured, respectively, in the present paper; the short-long-dashed curve is the pressure redshift of the central dip according to the mFCSM calculations in the present paper; the short-dashed curve is the PS of the central dip as in ApJ'87. The points, the shapes of which are not commented on here, are taken from different bibliographical sources and, as a rule, belong to other authors.

In Figure 5, we see that in ApJ'87 the PS values of the peak of the H_α Stark line profile are considerably overestimated. In the case of the H_β line, the circumstances are different. In Figure 6, it is clearly seen that the PSs of the central dip of H_β Stark line profiles were predicted well in ApJ'87, with a little excess as compared with the present, more precise data. The PSs measured by Wiese et al. (1972), presented in Figure 6, require a comment. We see that their best-fitting curve achieves zero electron concentration (i.e., the conditions of an isolated atom) at the blue PS of about 0.2 Å, which is, of course, not a reasonable result. Probably all these measurements of the H_β line were taken using temporarily defective recording equipment, producing unphysical, systematic (additive) redshift. (We see that Wiese's and our curves of the PS are nearly parallel.) When the presumed additive contribution (probably erroneous) is removed, the measurements by Wiese et al. precisely agree with our measurements and the modified-FCSM calculations.

5. THE EMERGING (SYNTHETIC) WD LINE PROFILE CALCULATIONS

Complete—broadened, asymmetrical, and shifted—Stark line profiles have been calculated for each layer of the WD atmosphere under examination, and subsequently convolved with the proper Doppler contribution. In Figures 7 and 8, we see, as an example, the final convolution of the Stark–Doppler effect for one of the shallowest layers (a relatively cool and rare one; Figure 7) and for one of the deepest (hot and dense) atmospheric layers (Figure 8).

The emerging (synthetic) Balmer line profile is a weighted mean, balanced by the transfer equation, of the contributions of all active, outer layers of the pure H model atmosphere. The superposition of the complete Stark–Doppler profiles of the H_β Balmer line (asymmetrical and redshifted), corresponding to successive atmospheric layers—from the extreme outer layer

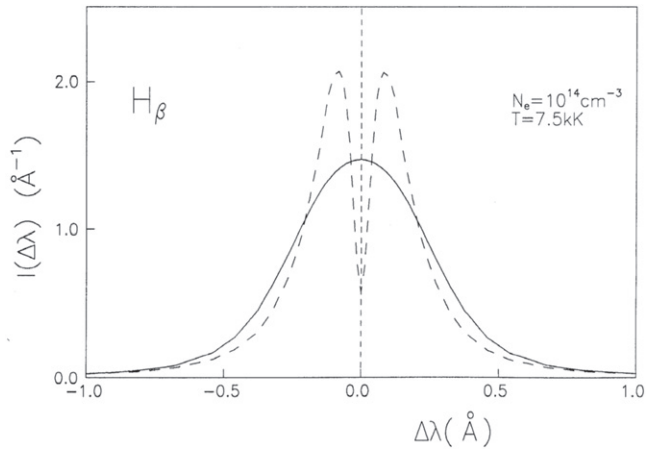

Figure 7. Stark H_β shape (the dashed line) and the final effect of the Stark–Doppler convolution (the solid line) in one of the shallowest WD atmospheric layers. We see that the final shape, given by the convolution operation, differs completely from the initial Stark shape. This is of the Doppler type, without any central structure.

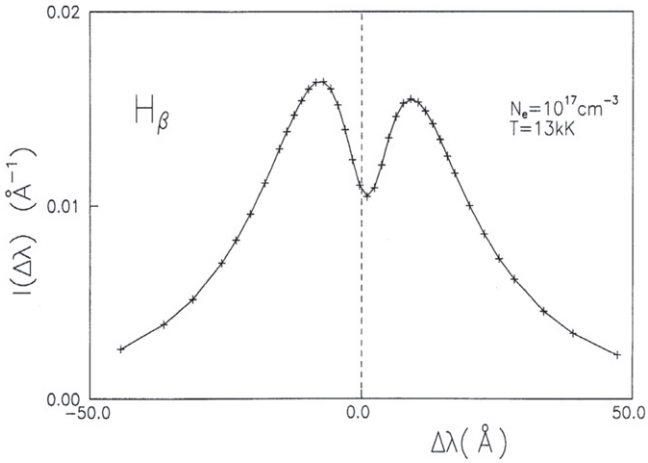

Figure 8. Stark H_β shape (the solid line) and the final effect of the Stark–Doppler convolution (crosses) in one of the deepest WD atmospheric layers. We see that the shape, given by the convolution operation, is identical with the initial Stark shape. In deep, hot, and dense atmospheric layers, where Stark broadening dominates totally, the contribution of the Doppler effect is completely negligible.

(narrow structure) down to the deepest one (extremely broad shapes)—is shown in Figures 9 and 10. (The H_α line was treated in just the same manner.)

In Figure 11(a), the synthetic spectrum in the region of the H_β line, calculated using opacity profiles, as in Figures 9 and 10, is presented on the flux scale. This "wide-angle" spectroscopic view is, of course, very similar to those observed via most advanced present-day instrumentation, as reported, e.g., by Barstow et al. (2001), Figure 4 therein, ground-based; Barstow et al. (2005), Figure 5 therein, *HST*; or Kepler et al. (2007), Figures 10 and 11 therein, SDSS.

Figure 11(b) shows the same, but on a reduced (0–1) scale, $r_\lambda = \mathrm{Flux_{line}/Flux_{continuum}}$. From the point of view of the gravitational redshift measurements, the clue lies in the line center—in the narrow central section, barely a few angstroms wide. We discuss the final results of the analysis of that region in detail in the next section.

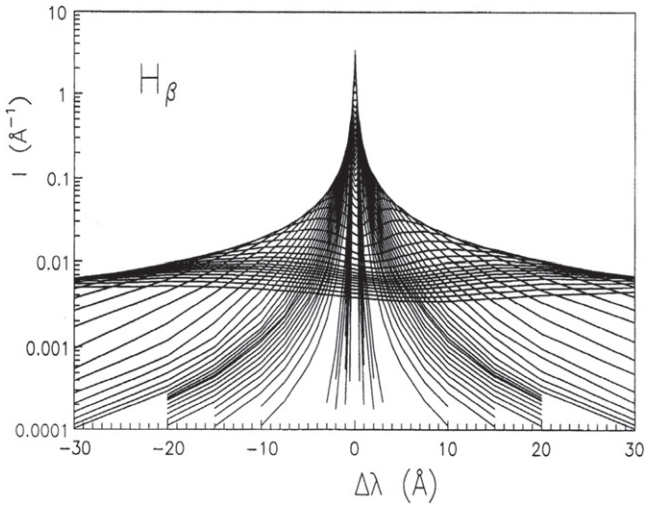

Figure 9. Superposition of the convolved Stark–Doppler profiles, corresponding to the successive WD atmospheric layers—from the outermost layers (the narrow, symmetrical, and unshifted shapes), down to the deepest ones (the extremely broad, asymmetrical, and redshifted shapes). The line-shape evolution is huge, indeed.

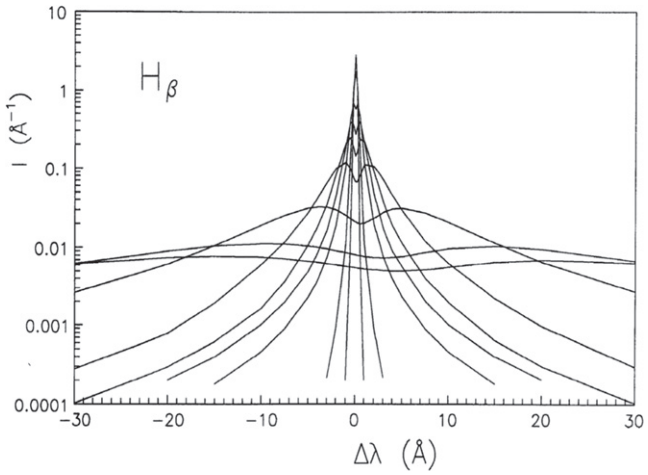

Figure 10. Same superposition as in Figure 9, but, for clarity, containing only a few line profiles (H_β opacity shapes) from selected atmospheric layers (every fifth one).

6. RESULTS AND CONCLUSIONS

The PS in the central parts of the synthetic H_α Balmer line is practically negligible; our earlier (ApJ'87) diagnosis in that matter is hereby confirmed. (N.B.: in conditions of very high-density plasma that scenery is more complicated—cf. the paper by Griem et al. (2005), e.g., Figures 9 and 13 therein—the PS of the H_α line achieves substantial values.) In the case of the synthetic H_β line, the central region is slightly affected by the PS, as correctly predicted in ApJ'87, but the near and far wings are affected enormously, as compared with ApJ'87. This is seen in our Figures 12 and 13, plotted on the basis of the synthetic spectra of the WD atmospheres of the typical parameters: $\log g = 8.0$ and $T_{\mathrm{eff}} = 12{,}000$ K (in figures we have used the abbreviation 12 kK), as an example.

We consequently use the concept of the pressure redshift of the WD Balmer lines as the redshift of the "ALC," introduced by Greenstein & Trimble (1967) to the WD spectra, and adapted in the experimental measurements, as the ELC paradigm, by Wiese & Kelleher (1971) and Wiese et al.

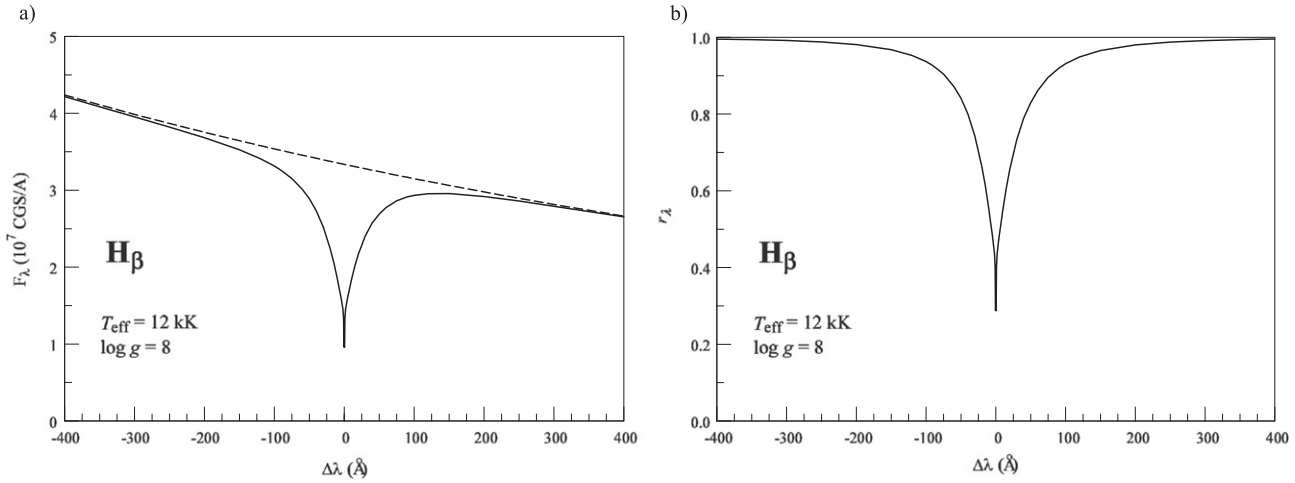

Figure 11. The synthetic spectrum in the region of the H_β line of a virtual WD of the given parameters, on the flux scale (left) and on the reduced (0–1) scale (right).

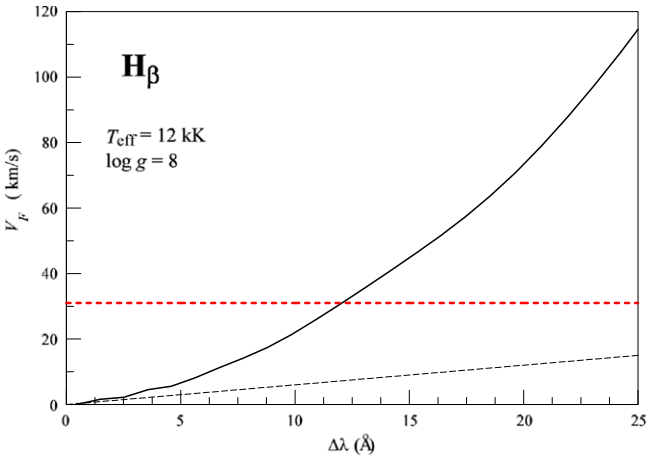

Figure 12. The Stark-induced shift (the pressure shift, PS) of the Balmer H_β line, in the ALC paradigm, of the WD atmosphere of the given parameters, as a function of the distance from the line center, on the flux scale. This figure has been generated on the basis of the diagram of the type of Figure 11(a). The solid line shows the present result, the thin dashed line that in ApJ'87. See the text for details. The dashed (horizontal) line represents approximately the level of the gravitational redshift in WDs of the parameters, as in the legend above—cf., e.g., Provencal et al. (1998); Falcon et al. (2010).

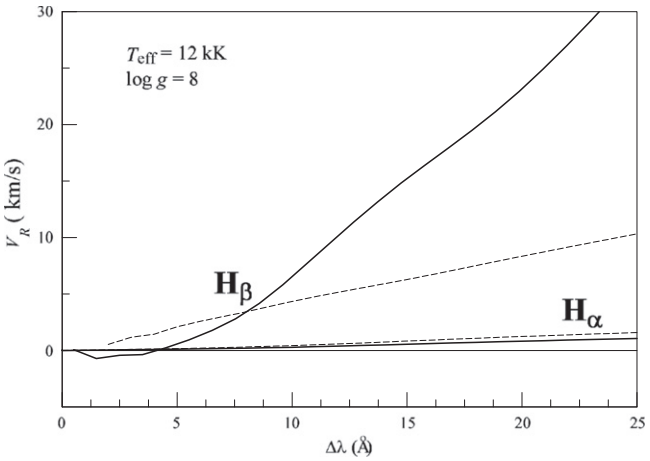

Figure 13. The main results of the present paper—the Stark-induced redshifts, expressed in units of the Doppler velocity, as functions of the distance from the line center, in the synthetic spectra of H_α and H_β Balmer lines of the WD of the given parameters. The diagram has been plotted on the basis of the synthetic Balmer line profiles, expressed in the residual intensities, r_λ, on a (0–1) scale of the type of Figure 11(b). See the text for details.

(1972). So, in Figures 12 and 13 the quantity $\Delta\lambda$ (Å) is used on the abscissa, and the pressure redshifts in the equivalent Doppler velocity units (v_F or v_r, respectively) on the ordinate, in conformity with the tradition in that subject. In Figure 12, the subscript F on the velocity symbol reminds that the ordinate axis of the synthetic WD spectrum is the flux scale F_λ (not the residual intensity r_λ). The thick curve in Figure 12 has been constructed by us from the WD synthetic spectrum, strictly in the same manner as an observer does on raw recording of the real WD spectrum. Here we must note, however, that the straightforward measurement of the WD gravitational redshift in the ALC convention can be falsified by apparent, "trivial" causes, the principal one of which is the redshift induced by the sloping of the Paschen continuum (cf., e.g., Schulz 1977). The measurements in the residual intensities, r_λ, on the (0–1) scale are free of that "trivial" contribution.

Figure 13 presents the main results of this paper—the Stark-induced redshift of the investigated Balmer lines for a WD of the given parameters—on the reduced scale, r_λ. We see here four curves. One pair of curves correspond to H_α, the other to the H_β line. The solid lines show new effects—the results of the present paper; the dashed ones refer to the results of ApJ'87, with the aim of comparing these results. Each of the dependences shown presents the Stark-induced redshift (PS) alone, i.e., the net pressure line shift (free of "trivial" contributions), produced by elementary physical processes in plasma of the WD atmosphere, in all its layers active in the formation—via the transfer equation—of the synthetic shape of a Balmer line.

We remember here the fundamental differences in the approaches applied in the earlier papers ApJ'87, A&A'90 and in the present paper: in the former ones, the symmetrical profiles of the Balmer lines, shifted as a whole, were used. The PS of the line center used at that time remains nearly correct. However, the synthetic line profiles—calculated at that time using symmetrical line profiles, shifted as a whole—have been uncertain. In the present paper, the Stark line profiles used are not only redshifted but also asymmetrical ones, similarly to those in real conditions. The results presented in Figure 13

permit us to formulate the following conclusions: (1) The Stark-induced redshift (PS) of the H_β line in WD spectra must be taken into account when measuring the gravitational redshift, especially in cases when the ALC paradigm is applied. In the H_β line in WD spectra, the Stark-induced redshift is far greater than that in the case of the H_α line; in the case of the latter, the pressure redshift can practically be neglected. (2) Our new values of the "observed" pressure redshift of the WD H_α line are nearly half those predicted in ApJ'87, whereas in the case of the WD H_β line they are considerably greater, especially at $\Delta\lambda > 10$ Å, than those in ApJ'87.

The effects of such clear differences in the observed features of both these lines, and in the resulting Stark-induced redshift in WD spectra, can be explained as a result of dissimilarity of the quantum structures of the two lines. The H_α line belongs to the so-called "odd" Balmer lines, with a strong central line component, whereas the H_β line is an "even" one, without the central component. These differences strongly manifest themselves in plasma spectroscopy in the laboratory (emissive, and thin-layer plasma; cf., e.g., Figures 3 and 4). In infinitely thick stellar atmospheres, the "odd–even" problem is—from the point of view of the observer—completely masked by processes of the transfer of radiation to outer layers of the stellar atmosphere and to the observer's eye: the synthetic lines of both these kinds have similar shapes, with a clearly formed central dip. In each atmospheric layer, however, the line shapes of opacities have such features as in a thin layer—cf. Figures 7–10 of the present paper.

The H_β line shape is a specific one (see Figures 4 and 8)—the red peak of the line is lower than the blue one (i.e., the "blue" opacity is greater than that in the "red" line region). Consequently, radiation transfer in the region of the red peak proceeds more easily than that in the blue peak. On the red side of the line, we "see" therefore more deep, dense, and hot layers, and on the blue side more shallow, relatively rare, and cool layers. These effects averaged (by a radiative transfer equation) produce additional (as compared with contribution of a single atmospheric layer) asymmetry and Stark-induced redshift of the synthetic line profile. The case of the H_α line is, due to a strong central component and nearly symmetrical Stark splitting, incomparably simpler: asymmetry effects (appearing in this line too) do not produce any substantial Stark-induced redshift.

When spectroscopic data of extremely high dispersion are available, e.g., from *HST* or VLT, and when the H_β line with the measurement of the central non-LTE dip (cf., e.g., Falcon et al. 2010, Figure 2, or Casewell et al. 2009, Figures 2 and 3) is used, the problem of the Stark-induced shift can be completely ignored. The non-LTE dip is formed in the uppermost, extremely rare atmospheric layers of a WD, where Stark effects are of no importance relative to the Doppler effect (cf. Figure 7). Here the observed line shift is entirely caused by the gravitational (Einstein's) effect. In more frequent cases of the middle-resolution spectra, for example from SDSS, (e.g., Kleinman et al. 2004; Madej et al. 2004; Kepler et al. 2007), the "average line center" defined in broader regions of the H_β line should be used for the gravitational redshift measurements. The same concerns the older archival spectroscopic data, often invaluable records of the past.

When the synthetic H_α or H_β Balmer line profiles in the residual intensity units, r_λ, on the (0–1) scale are used (as we see, e.g., in Figure 11(b)), the data from Figure 13, free of all "trivial" agents and the most reliable ones, should be used throughout.

We hope that the results presented here will be useful in a more precise determination of the gravitational redshifts in WD spectra and in a more accurate determination of the WD mass/radius ratio. It is important from the point of view of our understanding of WDs—objects that are widespread in Nature. Better knowledge of that ratio can also be helpful in imposing new limitations on the theory of the WD interior and can faciliate better calibration of Type Ia supernovae—exploding WDs in binary systems—and, consequently, can permit more precise examination of the density of dark matter in the universe.

J.M. acknowledges support by Polish National Science Centre grants No. 2011/03/B/ST9/03281 and 2013/10/M/ST9/00729.

REFERENCES

Baranger, M. 1958, PhRv, 111, 481
Barstow, M. A., Bond, H. E., Holberg, J. B., et al. 2005, MNRAS, 362, 1134
Barstow, M. A., Holberg, J. B., Hubeny, I., et al. 2001, MNRAS, 328, 211
Casewell, S. L., Dobbie, P. D., Napiwotzki, R., et al. 2009, MNRAS, 395, 1795
Djurović, S., Ćirišan, M., Demura, A. V., et al. 2009, PhRvE, 79, 046402
Edmonds, F. M., Schluter, D. C., & Wells, D. C. 1967, MmRAS, 7, 271
Falcon, R. E., Winget, D. E., Montgomery, M. H., & Williams, K. A. 2010, ApJ, 712, 585
Ferri, S., Calisti, A., Moss, C., et al. 2014, Atom, 2, 299
Gigosos, M. A., & Cardenoso, V. 1989, PhRvA, 37, 5258
Gigosos, M. A., & Cardenoso, V. 1996, JPhB, 29, 4795
Grabowski, B., & Halenka, J. 1975, A&A, 45, 159
Grabowski, B., Madej, J., & Halenka, J. 1987, ApJ, 313, 750
Greenstein, J. L., & Trimble, V. 1967, ApJ, 149, 283
Griem, H. R. 1964, Plasma Spectroscopy (New York: McGraw-Hill)
Griem, H. R. 1974, Spectral Line Broadening by Plasmas (New York: Academic)
Griem, H. R. 1983, PhRvA, 28, 1596
Griem, H. R., Halenka, J., & Olchawa, W. 2005, JPhB, 38, 975
Griem, H. R., Kolb, A. C., & Shen, K. Y. 1962, ApJ, 135, 272
Günter, S., & Könies, A. 1997, PhRvE, 55, 907
Halenka, J. 1990, ZPhyD, 16, 1
Halenka, J. 2009, EPJD, 53, 337
Halenka, J., & Olchawa, W. 1996, JQSRT, 56, 17
Halenka, J., & Olchawa, W. 2007, EPJD, 42, 425
Helbig, V., & Nick, K. P. 1981, JPhB, 14, 3573
Hubeny, I. 1988, CoPhC, 52, 103
Hubeny, I., & Lanz, T. 1997, http://nova.astro.umd.edu/Tlusty2002/pdf/tlguide195.pdf
Hubeny, I., & Lanz, T. 2000, http://nova.astro.umd.edu/Tlusty2002/pdf/syn43guide.pdf
Kepler, S. O., Kleinman, S. J., Nitta, A., et al. 2007, MNRAS, 375, 1315
Kepple, P., & Griem, H. R. 1968, PhRv, 173, 317
Kleinman, S. J., Harris, H. C., Eisenstein, D. J., et al. 2004, ApJ, 607, 426
Koester, D. 1987, ApJ, 322, 852
Madej, J. 1983, AcA, 33, 1
Madej, J., & Grabowski, B. 1990, A&A, 229, 467
Madej, J., Należyty, M., & Althaus, L. G. 2004, A&A, 419, L5
Olchawa, W. 2002, JQSRT, 74, 417
Olchawa, W., Olchawa, R., & Grabowski, B. 2001, in The PLASMA-2001, V International Symposium on Research and Applications of Plasmas, http://fizyka.uni.opole.pl/~wolch/P1.15.pdf
Olchawa, W., Olchawa, R., & Grabowski, B. 2004, EPJD, 28, 119
Provencal, J. L., Shipman, H. L., Hog, E., & Thejll, P. 1998, ApJ, 494, 759
Rausch von Traubenberg, H., & Gebauer, R. 1929a, ZPhy, 54, 307
Rausch von Traubenberg, H., & Gebauer, R. 1929b, ZPhy, 56, 256
Schulz, H. 1977, A&A, 54, 315
Trimble, V., & Greenstein, J. L. 1972, ApJ, 177, 441
Vidal, C. R., Cooper, J., & Smith, E. W. 1973, ApJS, 25, 37

Weidemann, V. 1979, in IAU Coll. 53, White Dwarfs and Variable Degeneratte Stars, ed. H. M. van Horn & V. Weidemann (Rochester: Univ. Rochester Press), 206
Wiese, W. L., & Kelleher, D. E. 1971, ApJ, 166, L59
Wiese, W. L., Kelleher, D. E., & Paquette, D. R. 1972, PhRvA, 6, 1132
Wujec, T., Olchawa, W., Halenka, J., & Musielok, J. 2002, PhRvE, 66, 066403